PFC/JA-85-8

Optimization of Gyroklystron Efficiency

T.M. Tran[a)], B.G. Danly, K.E. Kreischer,
J.B. Schutkeker and R.J. Temkin

Plasma Fusion Center
Massachusetts Institute of Technology
Cambridge, MA 02139

February 1985

This work was supported by the U.S. Department of Energy Contract No. DE-AC02-78ET51013.

[a)] Permanent address: CRPP, Association Euratom-Confédération Suisse, EPFL, 21, Av. des Bains, CH-1007 Lausanne, Switzerland

Optimization of Gyroklystron Efficiency

T.M. Tran[a)], B.G. Danly, K.E. Kreischer,

J.B. Schutkeker and R.J. Temkin

Plasma Fusion Center

Massachusetts Institute of Technology

Cambridge, MA 02139

ABSTRACT

In this paper, the optimization of gyroklystron efficiency is investigated by employing a two-step procedure. As a first step, the prebuncher is analyzed using a small signal approximation, since the cavity(ies) here serve mainly to modulate slightly the velocities of the electrons, which will be bunched in the field-free drift section(s). It is found that the electrons entering the energy extraction cavity can be characterized entirely by only two dimensionless parameters: a bunching parameter q and a relative phase ψ. The numerical simulation of the extraction cavity, based on the nonlinear pendulum equations describing the interaction between the electrons and the rf field, supplemented by the initial conditions specified by q and ψ, constitutes the second step. The final result of this two-step analysis is the efficiency, $\eta_{\perp,opt}$ optimized with respect to q, ψ and the magnetic detuning parameter Δ. This efficiency depends only on the normalized cavity length μ and the normalized rf field F of the energy extraction section. The efficiency as well as the conditions required to attain this optimum (q_{opt}, Δ_{opt}, and ψ_{opt}) are presented as contour plots on the (F, μ) plane and can be used efficiently to design gyroklystrons of any frequency and output power.

I. INTRODUCTION

In a single-cavity gyrotron, the energy extraction occurs in the same cavity as the phase bunching. However, for efficiency improvement, the multiple cavity gyrotron (or gyroklystron) may be advantageous because the electrons entering the energy extraction cavity have their phase angles properly bunched in the previous cavity(ies). In addition, mode locking by the prebunching cavity(ies) can be effective in the output cavity, which results in a stable single-mode operation.

Experiments with a two-cavity gyroklystron amplifier operating at 28 GHz were reported in Ref.1. An impressive gain of 40 dB was obtained, but only an efficiency of 10% was observed, probably due to spurious oscillations in the drift tube connecting the two cavities. Recently, Bollen *et al.*[2] reported efficiencies as high as 30% in their three-cavity gyroklystron, achieving a maximum output power of 51 kW.

The theoretical analysis of the gyroklystron usually consists of numerically integrating the equations of motion of the relativistic electrons subject to the rf fields in each cavity[3]. The main drawback of this brute force method is the large number of parameters (even for a two-cavity device) needed in the calculations, which prevents the extensive parametric studies of the gyroklystron efficiency that are necessary for optimum design. On the other hand, analytical small-signal calculations, based on Vlasov-Maxwell formalism[4] or on single-particle equations of motion[5] , although useful for providing some physical insights, are not sufficient for an accurate description of the gyroklystron performance.

In this paper, a linear approximation is used to analyse the electron phase bunching, which is shown to be characterized by a bunching parameter q. The nonlinear equations, describing the strong interaction between the beam and the rf fields in the energy extraction cavity are then solved numerically to obtain the output efficiency. Moreover, by

employing a normalization procedure well known in the Soviet gyrotron literature (see *e.g.*, Ref.6), an extensive parametric analysis is carried out for the gyroklystron operating at the fundamental. As a result, the optimum perpendicular efficiency of the gyroklystron, $\eta_\perp$, as well as the conditions for obtaining this optimum (the detuning parameter Δ, the bunching parameter q, and the relative phase of the rf field ψ), depend only on two parameters: the normalized length of the energy extraction cavity μ and the normalized beam current I (or the normalized rf field amplitude F). The results of this comprehensive analysis are very general and can be applied to the design of a gyroklystron of any frequency and power, operating either in the amplifier regime or in the locked oscillator mode. It should be noted that Ergakov *et. al* [7] have performed similar calculations for a two-cavity gyroklystron with feedback; the case we consider here has no feedback.

The paper is organized in the following manner. In Section II, the basic equations of the interaction between the beam and the rf fields, as well as the normalized parameters used in this paper, will be briefly summarized. In Section III, a linear analysis, based on these equations is done for the prebuncher of a two-cavity gyroklystron. Extension to the general multiple-cavity gyroklystron is also examined. Section IV is devoted to the discussion of the numerical results obtained by a nonlinear analysis of the energy-extraction cavity. Finally, the conclusions of this paper will be presented in Section V.

II. BASIC EQUATIONS

In Ref.8, Fliflet *et al.* gave a very detailed derivation of the slow time scale equations for an annular electron beam interacting with the circular TE_{mp} electric field given by

$$\mathbf{E}_t(r,\varphi,z,t) = \mathrm{Re}\left\{E_o\left(J'_m(k_\perp r)\hat{e}_\varphi + \frac{im}{k_\perp r}J_m(k_\perp r)\hat{e}_r\right)f(z)e^{i(\omega t - m\varphi)}\right\} \qquad (1)$$

where J_m is the Bessel function, $f(z)$ describes the axial profile of the rf field (normalized such that its maximum value is one) and $k_\perp$ is the transverse wave number

$$k_\perp = \nu_{mp}/R_o, \qquad (2.a)$$

where ν_{mp} is the p^{th} nonzero root of J'_m and R_o is the cavity radius; in gyrotron resonators

$$k_\perp \simeq k = \omega/c = 2\pi/\lambda \qquad (2.b)$$

In this derivation, a single-mode interaction and a weakly relativistic electron approximation ($n\beta_\perp^2/2 \ll 1$, where n is the cyclotron harmonic number) have been used. Furthermore, by redefining the dependent and independent variables according to (in the following, the subscript "o" denotes quantities at the entrance of the interaction region)

$$p = \gamma\beta_\perp/\gamma_o\beta_{\perp o}, \qquad (3.a)$$

$$\theta = n\phi - \omega t_o + \frac{\pi}{2}, \qquad (3.b)$$

$$\zeta = \frac{\pi\beta_{\perp o}^2}{\beta_{\parallel o}}\frac{z}{\lambda}, \qquad (3.c)$$

where ϕ is the *fast time scale* phase angle of the electron, t_o is the time when the electrons enter the interaction region and γ is the relativistic factor $\gamma = (1 - \beta_{\perp o}^2 - \beta_{\parallel o}^2)^{-1/2}$, it can be easily shown that the equations of motion for the electrons given in Ref.8 reduce

to the pendulum equations, also known as the Yulpatov equations in the Soviet gyrotron literature[6]

$$\frac{dp}{d\varsigma} = -Ff(\varsigma)p^{n-1}\sin\theta \tag{4.a}$$

$$\frac{d\theta}{d\varsigma} = -(\Delta + p^2 - 1) - nFf(\varsigma)p^{n-2}\cos\theta. \tag{4.b}$$

with $p(\varsigma_{in}) = 1$ and $\theta(\varsigma_{in}) = \theta_o$, θ_o being distributed over $[0, 2\pi]$. In this study, we use for f a fixed Gaussian profile given by

$$f(\varsigma) = e^{-(2\varsigma/\mu)^2} \tag{5}$$

In the energy extraction cavity, the limits $\varsigma_{in} = -\sqrt{3}\mu/2$ and $\varsigma_{out} = \sqrt{3}\mu/2$ are taken because they are a good approximation to actual tapered gyrotron resonators[6,11]. In the prebunching cavities, the same limits are chosen but, since linear theory applies for those cavities, the results are insensitive to the choice of limits. As a result, for a given initial distribution of θ_o, the system (4) is parametrized only by the normalized cavity length μ, the normalized field amplitude F and the frequency detuning parameter Δ defined by

$$\mu = \frac{\pi\beta_{\perp o}^2}{\beta_{\|o}}\frac{L}{\lambda} \tag{6.a}$$

$$F = \frac{E_o\beta_{\perp o}^{n-4}}{B_o c}\left(\frac{n^{n-1}}{2^{n-1}n!}\right)J_{m\pm n}(k_\perp R_e) \tag{6.b}$$

$$\Delta = \frac{2}{\beta_{\perp o}^2}\left(1 - \frac{n\omega_{co}}{\omega}\right) \tag{6.c}$$

where L is the cavity length, B_o is the static magnetic field, R_e is the beam radial position and $\omega_{co} = eB_o/\gamma_o m_e$ is the relativistic cyclotron frequency.

The perpendicular electron efficiency can be obtained by performing an average over the initial phase angles θ_o:

$$\eta_\perp = 1 - \left\langle p^2(\varsigma_{out})\right\rangle_{\theta_o} \tag{7}$$

The total electronic efficiency η_{el} is simply related to $\eta_\perp$ by $\eta_{el} = \left[\gamma_o \beta_{\perp o}^2 / 2(\gamma_o - 1)\right]\eta_\perp$. From Eq.(7) and Eq.(4.a), an alternative expression for $\eta_\perp$ can be written as

$$\eta_\perp = 2 \int_{\varsigma_{in}}^{\varsigma_{out}} F f \left\langle p^n \sin\theta \right\rangle_{\theta_o} d\varsigma \tag{8}$$

which expresses the energy conservation for the electrons in the electromagnetic field given by Eq.(1). By taking into account the balance between the power radiated by the electron beam and the losses (by diffraction through the cavity ends as well as by wall heating) of the system, a steady-state condition can be found. These losses can be characterized by a total quality factor Q. In terms of the dimensionless parameters defined in Eqs.(6), the power balance is expressed as

$$\eta_\perp I = F^2 \tag{9}$$

where I is the normalized current which is defined as follows (in the case where $f(\varsigma)$ is a Gaussian)

$$I = \left(\frac{2}{\pi}\right)^{\frac{5}{2}} \frac{eQI_A}{\epsilon_o \gamma_o m_e c^3} \beta_{\perp o}^{-2(3-n)} \left(\frac{\lambda}{L}\right) \left(\frac{n^n}{2^n n!}\right)^2 \frac{J_{m\pm n}^2(k_\perp R_e)}{(\nu_{mp}^2 - m^2) J_m^2(\nu_{mp})} \tag{10}$$

In Eq.(10), I_A is the beam current (in Amp.). There exists a starting condition for oscillations which can be derived from Eq.(9) as

$$I \geq I_{st} \equiv \lim_{F \to 0} \left(\frac{F^2}{\eta_\perp}\right) \tag{11}$$

In a single-cavity gyrotron where θ_o are uniformly distributed over $[0, 2\pi]$, $\eta_\perp$ can be calculated by solving Eq.(4), using the smallness of F and Eq.(8) or Eq.(7). This gives

$$I_{st}(\Delta, \mu) = \frac{4}{\pi \mu^2} \frac{e^{2x^2}}{\mu x - n}, \quad x \equiv \mu\Delta/4 \tag{12}$$

By using the kinetic approach, the same expression for I_{st} has been obtained[9]. For a given μ, the threshold for oscillations, I_{min}, can be defined as the minimum value of I_{st}:

$$I_{min}(\mu) = I_{st}(\Delta_{min}, \mu)$$

$$\Delta_{min} = 4\, x_{min}/\mu \tag{13}$$

$$x_{min} = 1/2\left(n/\mu + \sqrt{n^2/\mu^2 + 1}\right)$$

Therefore, in the 3-D parameter space (I, μ, Δ) of a gyromonotron, we can distinguish a region $I > I_{st}(\mu, \Delta)$ where at least one stable equilibrium point always exits, and the region $I_{min}(\mu) < I < I_{st}(\mu, \Delta)$, where stable equilibrium points may still be found. The latter region corresponds to the *hard excitation region*, while the former one is called *soft excitation region*, according to the known terminology employed in nonlinear oscillator theory (see *e.g.*, Ref.10). Extensive parametric studies, based on Eqs.(4–13) have been done[11,12] for a single-cavity gyrotron at cyclotron harmonic numbers n varying from one to five.

Finally, before closing this Section, it is interesting to note that a system of slow-time scale equations similar to Eqs.(4) can be formulated for a quasi-optical gyrotron operating in a TEM_{oo} mode, with the resonator axis (y-axis) oriented transverse to the electron beam axis (z-axis). By using Eqs.(3), one can show that the equations given in Ref.13 reduce to

$$\frac{dp}{d\varsigma} = -F\cos(ky_g - n\pi/2) f(\varsigma) p^{n-1} \sin\theta \tag{14.a}$$

$$\frac{d\theta}{d\varsigma} = -(\Delta + p^2 - 1) - nF cos(ky_g - n\pi/2) f(\varsigma) p^{n-2} \cos\theta. \tag{14.b}$$

where k is the wavenumber ($k = 2\pi/\lambda$), y_g is the coordinate of the electron guiding-center along the axis of the mirrors and $f(\varsigma)$ is still given by Eq.(5). Except for the detuning parameter Δ, the other dimensionless parameters should be modified according to

$$\mu = \frac{\beta_{\perp o}^2}{\beta_{\|o}} \left(\frac{2\pi w_o}{\lambda}\right) \tag{15.a}$$

$$F = \frac{E_o \beta_{\perp o}^{n-4}}{B_o c} \left(\frac{n^{n-1}}{2^{n-1} n!} \right) \tag{15.b}$$

$$I = \frac{2}{\pi^4} \frac{eQI_A}{\epsilon_o \gamma_o m_e c^3} \beta_{\perp o}^{-2(3-n)} \left(\frac{\lambda}{d} \right) \left(\frac{\lambda}{w_o} \right)^2 \left(\frac{n^n}{2^n n!} \right)^2 \tag{15.c}$$

Here, d is the mirror spacing and w_o is the radiation beam waist. For an annular beam ($y_g = R_e \sin\alpha$, $\alpha \in [0, 2\pi]$), an additional average over the electron guiding centers y_g should be done to obtain the efficiency for a quasi-optical gyrotron. However, for a pencil beam ($ky_g = \text{const.}$), Eqs.(14) are exactly the same as Eqs.(4). This implies that most of the results of this paper will be applicable for both waveguide and quasi-optical (in the pencil beam limit) gyrotrons.

III. LINEAR ANALYSIS

In a gyroklystron device, a prebuncher consists of a cavity followed by a drift section which is designed (in the ideal case) in such a way that no rf field can be excited. The prebuncher cavity serves mainly to modulate slightly the transverse momentum of the electron beam, and, due to the energy dependence of the relativistic mass of the electron, the inertial bunching mechanism will take place in the drift section. As a result, provided that the phase of the rf field of the energy extraction cavity has an appropriate value, the bunched electrons will interact efficiently with the cavity field. Additional cavities in the prebuncher can be useful in improving the bunching effects while keeping the length of the drift section as well as the field amplitude F in the cavities at a reasonably small value.

A. Two-cavity gyroklystron

Let us first consider the case of only one cavity in the prebuncher. Since F is small, the pendulum equations, Eqs.(4), describing the interaction between the electrons and the field can be integrated analytically by expanding p and θ in the small parameter F as follows

$$\begin{aligned} p &= p^{(0)} + p^{(1)} + \cdots \\ \theta &= \theta^{(0)} + \theta^{(1)} + \cdots \end{aligned} \tag{16}$$

where $p^{(k)}$ and $\theta^{(k)}$ contain F to the power of k (F^k). By inserting this expansion in Eqs.(4) with $n = 1$ (in the rest of this paper, only the fundamental cyclotron resonance is considered), we get the following system of linearized equations

$$\frac{dp^{(0)}}{d\zeta} = 0 \tag{17.a}$$

$$\frac{d\theta^{(0)}}{d\zeta} = -\left(\Delta + {p^{(0)}}^2 - 1\right) \tag{17.b}$$

$$\frac{dp^{(1)}}{d\zeta} = -Ff(\zeta)\sin\theta^{(0)} \tag{17.c}$$

$$\frac{d\theta^{(1)}}{d\varsigma} = -2p^{(0)}p^{(1)} - \frac{Ff(\varsigma)\cos\theta^{(0)}}{p^{(0)}} \qquad (17.d)$$

$$\vdots \qquad \vdots$$

The first two equations describe the unperturbed state of the electron beam

$$p^{(0)}(\varsigma) = 1 \qquad (18.a)$$

$$\theta^{(0)}(\varsigma) = \theta_o + \Delta(\varsigma_{in} - \varsigma) = \theta_c - \Delta\varsigma \qquad (18.b)$$

where θ_o (and consequently θ_c) are uniformly distributed over $[0, 2\pi]$. The Eq.(17.c) describes the electron momentum modulation by the rf field. Using Eq.(18.b) and the field profile given by Eq.(5), Eq.(17.c) can be easily integrated, and we obtain up to the first order in F

$$p(\varsigma_{out}) = p^{(0)}(\varsigma_{out}) + p^{(1)}(\varsigma_{out}) = 1 - \frac{\sqrt{\pi}}{2}F\mu G(x)\sin\theta_c \qquad (19)$$

where the function G is defined by

$$G(x) = \frac{2}{\sqrt{\pi}}\int_0^{\sqrt{3}} e^{-t^2}\cos(2xt)\,dt \simeq e^{-x^2}, \qquad (20)$$

and x is given by Eq.(12). Within the same order in the small parameter F, the bunching of the electron phase angles is given by Eq.(17.d). Adding the result readily obtained from this equation to Eq.(18.b), we get

$$\theta(\varsigma_{out}) = \theta_c - \frac{\sqrt{3}}{2}\mu\Delta + \frac{\sqrt{\pi}}{2}F\mu e^{-x^2}\left\{\sqrt{3}\mu\sin\theta_c + \mu x\cos\theta_c - \cos\theta_c\right\} \qquad (21)$$

The first two terms within the braces in Eq.(21) come from the integration of the first term in the RHS of Eq.(17.d) which describes the inertial bunching; the last term characterizes the force bunching. In most cases of interest, only the first inertial term dominates since μ is usually larger than one, and

$$|\,\mu x - 1\,| \ll 1 \qquad (22)$$

due to the requirements that the starting current I_{st} of the prebuncher cavity should be high in order to prevent self-oscillations [see Eq.(12)].

In the drift section, p remains constant (since $F = 0$ as pointed out at the beginning of this Section) and is equal to the RHS of Eq.(19). However, the phase angles θ evolve according to

$$\frac{d\theta}{d\zeta} = -\Delta_d + \sqrt{\pi} F_1 \mu_1 e^{-x_1^2} \sin\theta_c \tag{23}$$

Here, the subscripts "1" and "d" have been introduced to denote quantities defined respectively in the first cavity and in the drift section. The bunched phase angles of the electrons at the end of the drift section (of length μ_d) can be obtained by solving Eq.(23) with the initial condition specified by Eq.(21)

$$\theta_b = \theta_c - \left(\frac{\sqrt{3}}{2} \mu_1 \Delta_1 + \mu_d \Delta_d \right) + q \sin\theta_c \tag{24.a}$$

$$q = \sqrt{\pi} F_1 \mu_1 e^{-x_1^2} \left(\frac{\sqrt{3}}{2} \mu_1 + \mu_d \right) \tag{24.b}$$

where the approximation (22) has been used to drop the term proportional to $\cos\theta_c$. This expression differs from the one employed in Refs.13 and 14 only by the additional bunching term $\sqrt{3}\mu_1/2$ which is retained here to deal with the case $\mu_d \simeq \mu_1$.

As a result, the electron phase angles, at the input of the second cavity, can be parametrized by a bunching parameter q which is defined in terms of the characteristics of the prebuncher, and a constant phase ψ which accounts for the phase difference between the cavities and the electron rotational drift [$\mu\Delta$ terms in Eq.(24.a)]

$$\theta_{o,2} = \theta_c + q \sin\theta_c - \psi \tag{25}$$

In the case of a Sine profile ($f(\zeta) = \sin(\pi\zeta/\mu)$, $0 \le \zeta \le \mu$), the bunched angles $\theta_{o,2}$ are still given by Eq.(25), provided the bunching parameter q is appropriately defined by

$$q = \frac{4\pi \cos(\mu_1\Delta_1/2)}{\pi^2 - \mu_1^2\Delta_1^2} F_1 \mu_1 \left[\mu_d + \frac{\mu_1}{4} - \frac{\mu_1^2 \Delta_1}{\pi^2 - \mu_1^2\Delta_1^2} \tan\left(\frac{\mu_1\Delta_1}{2} \right) \right]$$

Negecting the bunching effect in the cavity ($\mu_1 \ll \mu_d$), we recover the expression given in Ref.1.

The small-signal efficiency in the second cavity can be calculated by solving the linearized equations (17) with the initial conditions specified by Eqs.(19) and (25). To the first order in F_1 and F_2, the transverse momentum at the output of the second cavity is

$$p_{out,2} = 1 - \frac{\sqrt{\pi}}{2} F_1 \mu_1 e^{-x_1^2} \sin\theta_c - \frac{\sqrt{\pi}}{2} F_2 \mu_2 e^{-x_2^2} \sin\left[\theta_{o,2} - \frac{\sqrt{3}}{2}\mu_2 \Delta_2\right] \tag{26}$$

Making use of Eqs.(7),(25) and (26), we obtain

$$\eta_\perp^{lin} = \sqrt{\pi} F_2 \mu_2 e^{-x_2^2} \int_0^{2\pi} \sin\left[\theta_c + q\sin\theta_c - \psi - \frac{\sqrt{3}}{2}\mu_2\Delta_2\right] \frac{d\theta_c}{2\pi} \tag{27}$$

since $\langle \sin\theta_c \rangle_{\theta_c} = 0$. The integration yields finally

$$\eta_\perp^{lin} = \sqrt{\pi} F_2 \mu_2 e^{-x_2^2} J_1(q) \sin(\psi + \frac{\sqrt{3}}{2}\mu_2\Delta_2) \tag{28}$$

where J_1 is the first order Bessel function. From the definition of the starting current, Eq.(11), one can deduce that, provided q has a nonzero value,

$$I_{st,2} = 0 \tag{29}$$

for the second cavity. For any given current I_2, the cavity will oscillate and, using the power balance, Eq.(9), the field amplitude F_2 is given by

$$F_2 = \sqrt{\pi} I_2 \mu_2 e^{-x_2^2} J_1(q) \sin(\psi + \frac{\sqrt{3}}{2}\mu_2\Delta_2) \tag{30}$$

The optimum efficiency in the small-signal regime will take place when

$$q = q_{opt} = 1.84 \tag{31.a}$$

$$\Delta_2 = \Delta_{2,opt} = 0 \tag{31.b}$$

$$\psi = \psi_{opt} = \frac{1}{2}\pi,\ \frac{5}{2}\pi, \ldots \tag{31.c}$$

$$\text{and is equal to} \qquad \eta_{\perp,opt} = 1.03\, F_2\mu_2 \tag{31.d}$$

As will be found in the Section IV where nonlinear calculations will be performed, values of q_{opt} even higher than 1.84 are required to obtain optimum energy extraction in the strong field F region. Although one can achieve arbitrarily high values for the bunching parameter by choosing the operating Δ_1 and μ_1 close enough to the starting current I_{st} of the first cavity (in order to obtain high F_1), it can result in a very unstable operation because small perturbations of the device parameters such as the magnetic field or the beam current lead to large changes in q. On the other hand, increasing the prebuncher length to increase q [see Eq.(24.b)] could deteriorate the electron bunching in the drift section, due to the effects of the electron velocity spread[1,3]. From these considerations, the power needed to drive the first cavity must be sufficient to attain the desired value of q for optimum efficiency of energy extraction and stable operation. This power can be fairly high in some cases. In order to alleviate this constraint, a gyroklystron with many prebuncher cavities will be considered.

B. Multiple cavity gyroklystron

The analysis of such a scheme can be done by a straightforward extension of the previous one. In this analysis, we assume that there is modest gain from cavity to cavity except for the last (energy extraction) cavity, and that linear theory can be used to describe each cavity in the prebuncher. We also assume that the inertial bunching dominates over the force bunching. Solving successsively the linearized equations, Eqs.(17), for each cavity and the field-free pendulum equations, Eqs.(4), for each drift section, the normalized momentum at the output of the j^{th} cavity, $p_{out,j}$, and the phase angles at the midplane of the $(j+1)^{th}$ following cavity, $\theta_{c,j+1}$ can be expressed as

$$p_{out,j} = 1 - \frac{\sqrt{\pi}}{2} \sum_{k=1}^{j} F_k \mu_k e^{-x_k^2} \sin \theta_{c,k} \qquad (32.a)$$

$$\theta_{c,j+1} = \theta_{c,j} + \widehat{\mu}_{d,j} \sum_{k=1}^{j} \frac{q_k}{\widehat{\mu}_{d,k}} \sin\theta_{c,k} - \widehat{\psi}_j, \qquad j = 1, \ldots, N-1 \tag{32.b}$$

where

$$\widehat{\mu}_{d,j} = \frac{\sqrt{3}}{2}\mu_j + \mu_{d,j}, \tag{33.a}$$

$$q_j = \sqrt{\pi} F_j \mu_j \widehat{\mu}_{d,j} e^{-x_j^2}, \tag{33.b}$$

$$\widehat{\psi}_j = \frac{\sqrt{3}}{2}\mu_j \Delta_j + \mu_{d,j}\Delta_{d,j} + \frac{\sqrt{3}}{2}\mu_{j+1}\Delta_{j+1} + (\psi_{j+1} - \psi_j), \tag{33.c}$$

and N is the total number of cavities in the gyroklystron (the N^{th} cavity is the energy extraction cavity). In Eq.(33.c), ψ_j denotes the rf field phase in cavity j, while $\widehat{\psi}_j$ is the difference of phases between cavity $j+1$ and j, plus the rotational drift of the electron from the midplane of cavity j to the midplane of cavity $j+1$. With $\theta_{c,1}$, which is the electron phase angle at the center of the first cavity and therefore, is uniformly distributed over $[0, 2\pi]$, Eqs.(32) describe completely the electron bunching process. At the input of the last (energy extraction) cavity, the electron phase angles are simply given by

$$\theta_{o,N} = \theta_{c,N} + \frac{\sqrt{3}}{2}\mu_N \Delta_N \tag{34}$$

The complexity of the expressions in Eqs.(32) can be greatly reduced by assuming that

$$q_1 < q_2 < \cdots < q_{N-2} < 1 \tag{35}$$

which is consistent with a modest gain in successive prebuncher cavities. As a result, we obtain from Eq.(32.b) the same simple expression for the electron bunching, as the one in a two-cavity gyroklystron:

$$\theta_{c,j+1} = \theta_{c,1} + q_j \sin\theta_{c,1} - \widehat{\psi}_j, \qquad j = 1, \ldots, N-1 \tag{36}$$

Repeating the calculations which lead to Eq.(30), with the aid of Eq.(33.b), it is straightforward to get

$$F_j = \frac{\sqrt{\pi}}{2} I_j \mu_j e^{-x_j^2} q_{j-1} \sin \widehat{\psi}_j \tag{37.a}$$

$$\frac{q_j}{q_{j-1}} = \frac{\pi}{2} I_j \mu_j^2 \widehat{\mu}_{d,j} e^{-2x_j^2} \sin \widehat{\psi}_j, \qquad j = 2, \ldots, N-1 \tag{37.b}$$

where the approximation $J_1(q) \simeq q/2$ has been used. The bunching parameter q_1, produced by the first cavity can be determined simply by invoking the power balance between the input power, the power absorbed (or emitted) by the electron beam and the power lost by the cavity (wall heating, diffraction). The requirement that the first cavity does not self oscillate is fulfilled if $I_1 \leq I_{min,1}$, where $I_{min,1}$ is the threshold current defined in Eqs.(12) and (13). Thus, using q_1 and Eqs.(37), the field amplitude and bunching parameter can be obtained in successive cavities by iteration. The equation (36) then gives the input bunched phase angles for the electrons entering the final (energy extraction) cavity.

In the case of constant guiding magnetic field and identical sizes for the buncher cavities as well as for the drift sections

$$\begin{aligned} I_1 &= \cdots = I_{N-1} = I_B, \\ \mu_1 &= \cdots = \mu_{N-1} = \mu_B, \\ \mu_{d,1} &= \cdots = \mu_{d,N-1} = \mu_D, \\ x_1 &= \cdots = x_{N-1} = x_B, \end{aligned} \tag{38}$$

an upper limit for q_j/q_{j-1} can be written as

$$\frac{q_j}{q_{j-1}} \leq \frac{\pi}{2} I_B \mu_B^2 \widehat{\mu}_D e^{-2x_B^2} \tag{39}$$

For a given μ_B, the first cavity will operate in an absorption regime when the frequency detuning is small ($x_B \leq 1/\mu_B$ or $\Delta_B \leq 4/\mu_B^2$); this results in a very small initial bunching

parameter q_1. Therefore, the overall efficiency of bunch formation would be very poor, although the RHS of Eq.(39) is maximum for $x_B = 0$. On the other hand, the positive contribution from the electrons becomes maximum when Δ_B approaches the value given by $x_B = x_{min,1}$, provided $I_B < I_{min,1}$. For example, taking $I_B = 0.8\, I_{min,1}$, $\mu_B = \mu_D = 3$ (which corresponds for instance to a 80 kV electron beam, a velocity ratio $\alpha = 1.5$ and length ratio $L/\lambda = 1.5$), the maximum multiplication factor q_j/q_{j-1} can be as high as 8 (power gain of 18 dB per stage) if $x_B = x_{min,1}$.

As a final remark, we should mention that a detailed analysis of Eq.(32.b) reveals that a better bunched electron beam can be formed when q_j have the same order of magnitude, *i.e.*, when the inequality (35) does not apply. Such a regime of operation can result in a somewhat higher efficiency at the expense of a lower gain. The analysis of this case, however, will not be carried out further in this paper.

In summary, from the linear analysis, after traversing the prebuncher consisting of one or several cavities, the bunched electron beam can be modelled by only two parameters as follows

$$p_{in} = 1, \tag{40.a}$$

$$\theta_{in} = \theta_c + q \sin\theta_c - \psi, \qquad \theta_c \textit{ uniformly distributed over } [0, 2\pi], \tag{40.b}$$

at the input of the energy extraction cavity. The modulation terms [see Eq.(32.a)] have been neglected in Eq.(40.a) since the rf field in this cavity is much stronger than in the previous ones for high energy extraction efficiency. Then, by a numerical optimization of the nonlinear efficiency based on Eqs.(4), (7) and (40), we readily obtain the desired values of q and ψ, necessary for design of the prebuncher. This will be examined in detail in the next Section.

IV. NONLINEAR ANALYSIS

As the bunched electrons flow through the energy extracting cavity, a strong interaction between the electrons and the resonator rf field will take place if the field phase has an adequate value. The mechanism of this interaction is described by the nonlinear pendulum equations (4) and the initial conditions (40). A more convenient form (suitable for a numerical treatment) for these equations can be written as

$$\frac{dP}{d\zeta} = i\left(\Delta - 1 + |P|^2\right) P + iFf(\zeta) \tag{41.a}$$

$$P(\zeta = \zeta_{in}) = e^{-i(\theta_c + q\sin\theta_c - \psi)}, \quad \theta_c \textit{ uniformly distributed over } [0, 2\pi] \tag{41.b}$$

in the fundamental cyclotron harmonics ($n = 1$) case. A Gaussian profile defined by Eq.(5) will be used to model $f(\zeta)$ in all the following calculations. The perpendicular efficiency is simply defined by

$$\eta_\perp = \eta_\perp(F, \mu, \Delta, q, \psi) = 1 - \int_0^{2\pi} |P(\zeta = \zeta_{out})|^2 \frac{d\theta_c}{2\pi} \tag{42}$$

The efficiency $\eta_\perp$, as a function of q and ψ is determined in two steps. First, Eq.(41.a) is integrated (using a first order predictor-corrector method) for an unbunched beam, *e.g.* with a set of initial angles $\theta_{in} = \theta_c$ uniformly distributed over $[0, 2\pi]$, to tabulate $P(\zeta = \zeta_{out})$ versus θ_c. Then, by employing a linear interpolation from these tabulated data, $\eta_\perp$ is calculated from Eq.(42) for any pair (q, ψ). By this method, we perform the integration of (41.a) only once for any given set of q and ψ. (This method is virtually the same as the one employed in Ref.13 to investigate the quasi-optical gyroklystron).

A numerical optimization follows in order to determine the maximum of $\eta_\perp$ with respect to q and ψ. A further optimization versus Δ results finally to the optimum efficiency

as well as the optimum conditions which depend only on F and μ as follows

$$\begin{aligned} \eta_{\perp,opt} &= \eta_{\perp,opt}(F,\mu) \\ \Delta_{opt} &= \Delta_{opt}(F,\mu) \\ q_{opt} &= q_{opt}(F,\mu) \\ \psi_{opt} &= \psi_{opt}(F,\mu) \end{aligned} \tag{43}$$

$$\text{and} \qquad \frac{\partial \eta_\perp}{\partial \Delta} = \frac{\partial \eta_\perp}{\partial q} = \frac{\partial \eta_\perp}{\partial \psi} = 0 \quad \text{at } \Delta_{opt},\, q_{opt},\, \psi_{opt} \tag{44}$$

Using the power balance, Eq.(9), the independent variables F, μ in Eq.(43) can be transformed numerically to I, μ in order to obtain the operating conditions for a given current and a cavity length.

The equation (41.a) was integrated for 128 particles with different θ_c distributed equidistantly in $[0, 2\pi]$ and 256 intervals on an equidistant ς-mesh have been used to obtain reasonable accuracy in $\eta_\perp$ calculations. Agreement with the results derived in the weak-field limit, Eqs.(31), is found to be excellent for $F < 0.02$ and μ satisfying $F\mu < 0.2$. The alternative expression for $\eta_\perp$ (8) has been used for higher F values as a diagnostic for the numerical integration.

The contour plots of $\eta_{\perp,opt}$, Δ_{opt}, q_{opt} and ψ_{opt} in the (F,μ) plane are depicted in Figs.1. Efficiency as high as 90.8% has been found for $F = 0.14$ and $\mu = 15.5$ provided that $\Delta_{opt} = 0.538$, $q_{opt} = 3.17$ and $\psi_{opt} = 0.84\,\pi$. As shown in Fig.1c, the optimum q in the high field region is slightly higher than the value of 1.84 found in the linear regime, due to the presence of higher order terms in F in the expression of $\eta_\perp$.

Another feature of interest in Fig.1a is that the region where the efficiency is greater than 80% is fairly extensive in the (F,μ) plane. Notice that this level of efficiency is not accessible in a gyromonotron (unbunched beam) where the same Gaussian profile is assumed. Furthermore, when compared to the isoefficiency curves of a gyromonotron,

shown in Fig.2, it is interesting to note that the high efficiency contours of a gyroklystron migrate towards the low F and μ region, as a result of the prebunching effects. One important implication of this, as discussed in Ref.15 is the possibility of lower order mode operation in high frequency ($\geq$ 100 GHz) and high power ($\geq$ 1 MW) gyroklystrons.

For very high field amplitude F, the optimum efficiency exhibits a second maximum in the (F, μ) plane. In that region, after a rapid deceleration stage, the electrons can regain energy from the rf field before yielding again their energy to the rf field towards the output end of the cavity while in the low F region (including the first efficiency maximum), the energy transfer from the electrons is always a monotone increasing function of ς, once the "bunch" has been formed. It is interesting to observe that the transition between these two regimes occurs in a region of the (F, μ) plane where the change in $\eta_\perp$ is smooth but the change in q and ψ is very steep. This is explained by the jump of the optimum values of q and ψ from one local maximum to another local maximum of the efficiency in the (q, ψ) plane as the field amplitude F increases across the transition region.

In Fig.3, the isoefficiency curves are shown in the (I, μ) plane. Also shown in this figure (dashed line), is the curve $I_{min}(\mu)$ which is defined in Eqs.(12) and (13). For $I < I_{min}$ no oscillations are expected unless the electron beam is prebunched. (In a gyromonotron, the I_{min}-curve is precisely the $\eta_\perp = 0$ isoefficiency contour). In this region, which can be referred to as the *amplifier* regime, high efficiency occurs for a short cavity length and near the boundary $I = I_{min}$ where efficiency higher than 60% can be obtained for $\mu \leq 7$. Higher efficiency can be reached in the $I > I_{min}$ region which can be referred to as the *locked oscillator* regime since the cavity can still oscillate even when the prebunching is turned off. From Fig.3, it can be seen that the maximum efficiency peak of 90.8%, mentioned above requires a beam current 16.7 times higher than I_{min}. The next efficiency peak occurs

at $\mu = 22$ and $I = 193\, I_{min}$. Such large currents could lead to problems regarding the stability of the working mode against competing parasitic modes[16].

V. CONCLUSION

From a linear analysis of the prebuncher where the weak-field approximation can be assumed, a simple two parameter model for the bunched electron beam was derived for a two-cavity gyroklystron. For a multiple-cavity device designed such that the gain per stage is modest, we have shown that the bunching can also be described by only two parameters. A major result from the analysis of such device is the possibility of large gain enhancement by additional prebuncher cavities in a gyroklystron operating as an amplifier.

Utilizing the bunching model derived from linear theory, a thorough optimization was then carried out to determine the optimum efficiency of energy extraction in the output cavity, as a function of the normalized field amplitude F and the normalized (output) cavity length μ. This optimum efficiency, as well as the different optimum parameters were presented in a convenient graphical form in Figs.1 and 3, from which design studies (such as the ones discussed in Ref.15 for a single-cavity gyrotron) can be performed efficiently for gyroklystrons of any frequency and output power. Furthermore, these results can be applicable for a quasi-optical gyroklystron when the electron beam radius is much smaller than the radiation wavelength (pencil beam), as pointed out in Section II.

The influences of the electron velocity spread (hot beam) and the space-charge field on the gyroklystron performance were not considered in this paper. However, the effect of velocity spread can be easily simulated by solving the pendulum equations (4) for a population of electrons having different velocities. The influence of the space-charge field can be taken into account by including an additional force term in the RHS of Eqs.(4) as shown by Bratman and Petelin[17]. For a specific gyroklystron design, these additional calculations would be complementary to the performance curves obtained in this paper.

As a final remark, this two-step technique can be employed to analyze other devices

based on prebunching of the beam such as the gyrotwystron. It can also be extended to the harmonic operation of these devices.

ACKNOWLEDGEMENTS

This work was supported by the U.S. Department of Energy Contract No. DE-AC02-78ET51013 and in part by the Office of Naval Research. One of the authors (T.M.T.) would like to acknowledge the support received from the Swiss National Science Foundation.

REFERENCES

[a] Permanent address: CRPP, Association Euratom-Confédération Suisse, EPFL, 21, Av. des Bains, CH-1007 Lausanne, Switzerland

[1] R. S. Symons and H. R. Jory, in *Advances in Electronics and Electron Physics*, edited by C. Marton (Academic Press, New York, 1979) vol. 1, pp. 1–54.

[2] W. M. Bollen, A. K. Ganguly, B. Arfin, C. Sedlak, and R. K. Parker, *IEDM Digest*, 1984, paper 35.5, p. 838.

[3] A. K. Ganguly and K. R. Chu, *Int. J. Electron.* **51**, 503(1981).

[4] M. Caplan, *Conf. Dig., Eigth Int. Conf. on Infr. and Mm. Waves*, Florida, 1983, IEEE Cat. No. 83CH1917-4, paper W4.2.

[5] A. K. Ganguly and A. W. Fliflet, *Conf. Dig., Ninth Int. Conf. on Infr. and Mm. Waves*, Takarazuka, 1984, paper W.2.1, p. 227.

[6] V. A. Flyagin, A. L. Gol'denberg, and G. S. Nusinovich, in *Infrared and Millimeter Waves*, edited by K.J. Button (Academic Press, New York, 1984) vol.11, pp. 179–226.

[7] V. S. Ergakov, M. A. Moiseev and R. É. Érm, *Radiophys. Quantum Electron.* **22**, 700(1979).

[8] A. W. Fliflet, M. E. Read, K. R. Chu, and R. Seeley, *Int. J. Electron.* **53**, 505(1982).

[9] K. E. Kreischer and R. J. Temkin, in *Infrared and Millimeter Waves*, edited by K.J. Button (Academic Press, New York, 1983) vol. 7, pp. 377–485.

[10] N. N. Bogolyubov and Y. A. Mitropolsky, *Asymptotic methods in the theory of non-linear oscillations*, (Hindustan Publishing Corpn. India, 1961), pp.91–104.

[11] G. S. Nusinovich, and R. É. Érm, *Elektron. Tekh., Ser. 1, SVCh Elektronika* **8**, 55(1972).

[12] B. G. Danly, MIT Plasma Fusion Center Report No. PFC/JA-85-6, 1985.

[13] A. Bondeson, W. M. Manheimer and E. Ott, in *Infrared and Millimeter Waves*, edited by K.J. Button (Academic Press, New York, 1983) vol. 9, pp. 309–340.

[14] V. S. Ergakov and M. A. Moiseev, *Radiophys. Quantum Electron.* **1**, 89(1975).

[15] K. E. Kreischer, B. G. Danly, J. B. Schutkeker and R. J. Temkin, MIT Plasma Fusion Center Report No. PFC/JA-84-43, 1984.

[16] V. S. Ergakov, M. A. Moiseev and R. É. Érm, *Radiophys. Quantum Electron.* **3**, 318(1976).

[17] V. L. Bratman and M. I. Petelin, *Radiophys. Quantum Electron.* **18**, 1136(1975).

FIGURE CAPTIONS

Figure 1a The gyroklystron perpendicular efficiency $\eta_\perp$, optimized with respect to Δ, q and ψ, versus the normalized field amplitude F and the normalized cavity length μ.

Figure 1b The optimum frequency detuning parameter Δ.

Figure 1c The optimum bunching parameter q.

Figure 1d The optimum relative phase ψ.

Figure 2 The gyromonotron ($q = 0$) perpendicular efficiency $\eta_\perp$, optimized with respect to Δ, versus the normalized field amplitude F and the normalized cavity length μ.

Figure 3 The gyroklystron perpendicular efficiency $\eta_\perp$, optimized with respect to Δ, q and ψ, versus the normalized beam current I and the normalized cavity length μ. The dashed line represents the threshold current I_{min} for an unbunched beam.

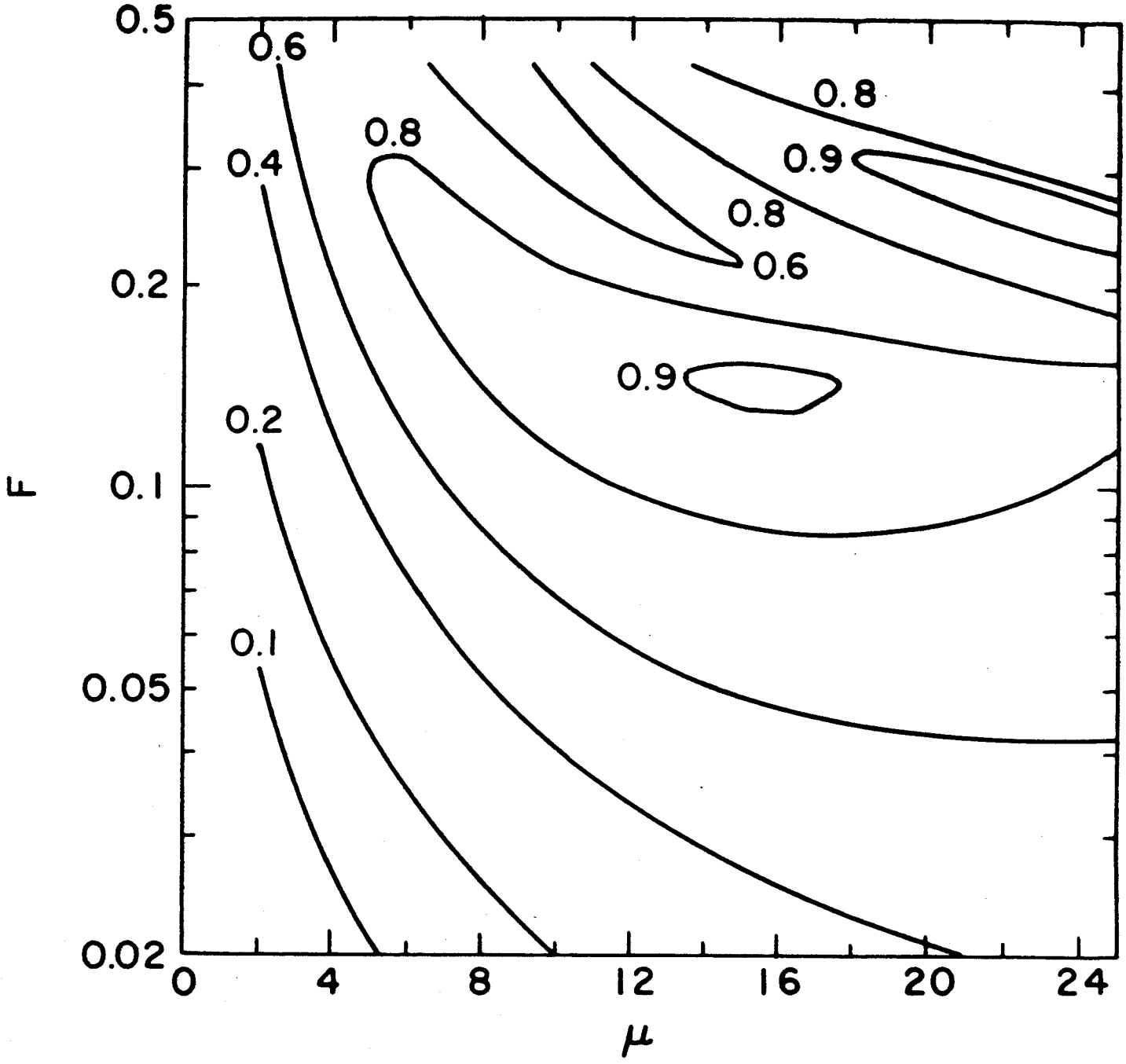

Figure 1a

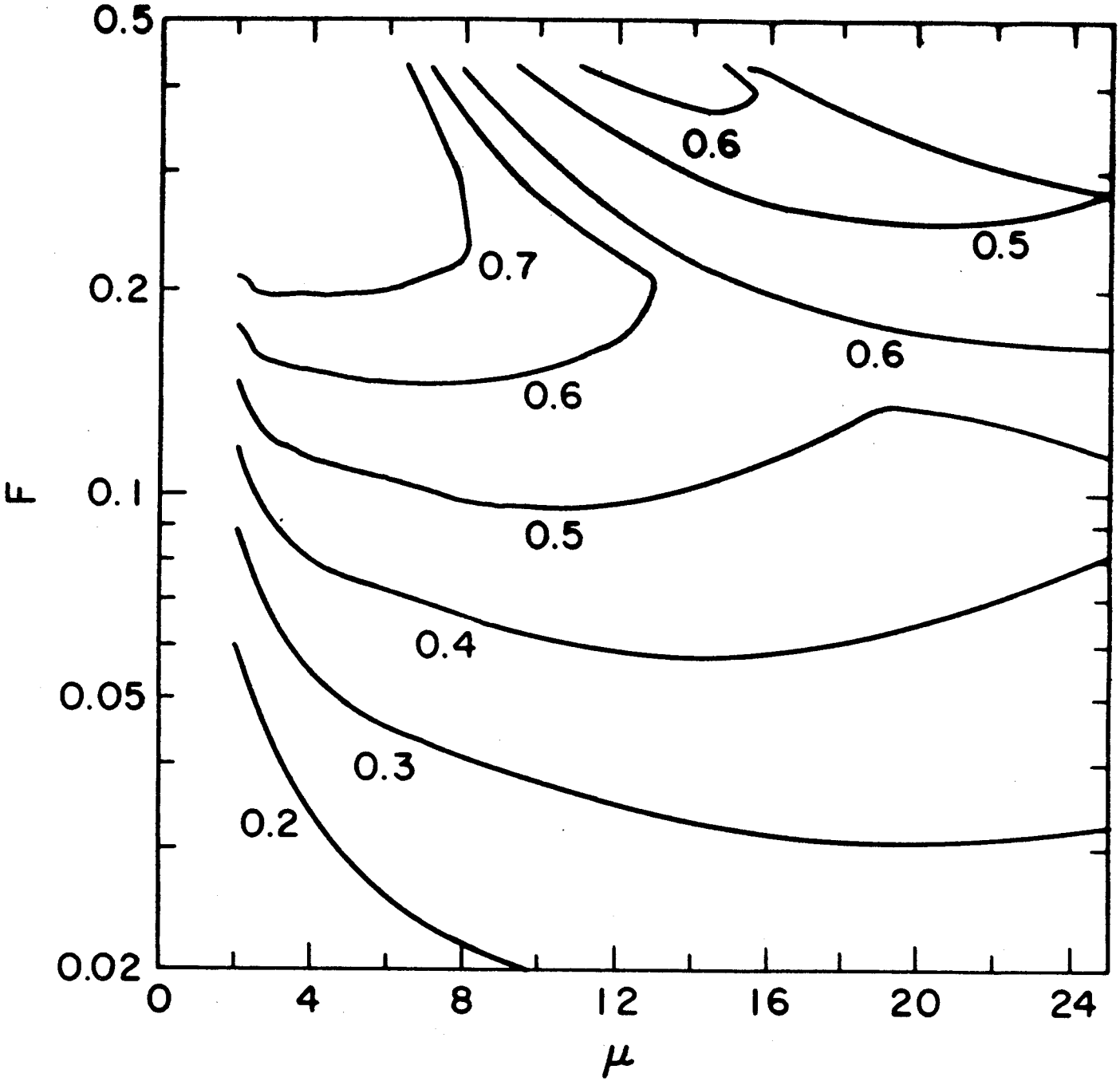

Figure 1b

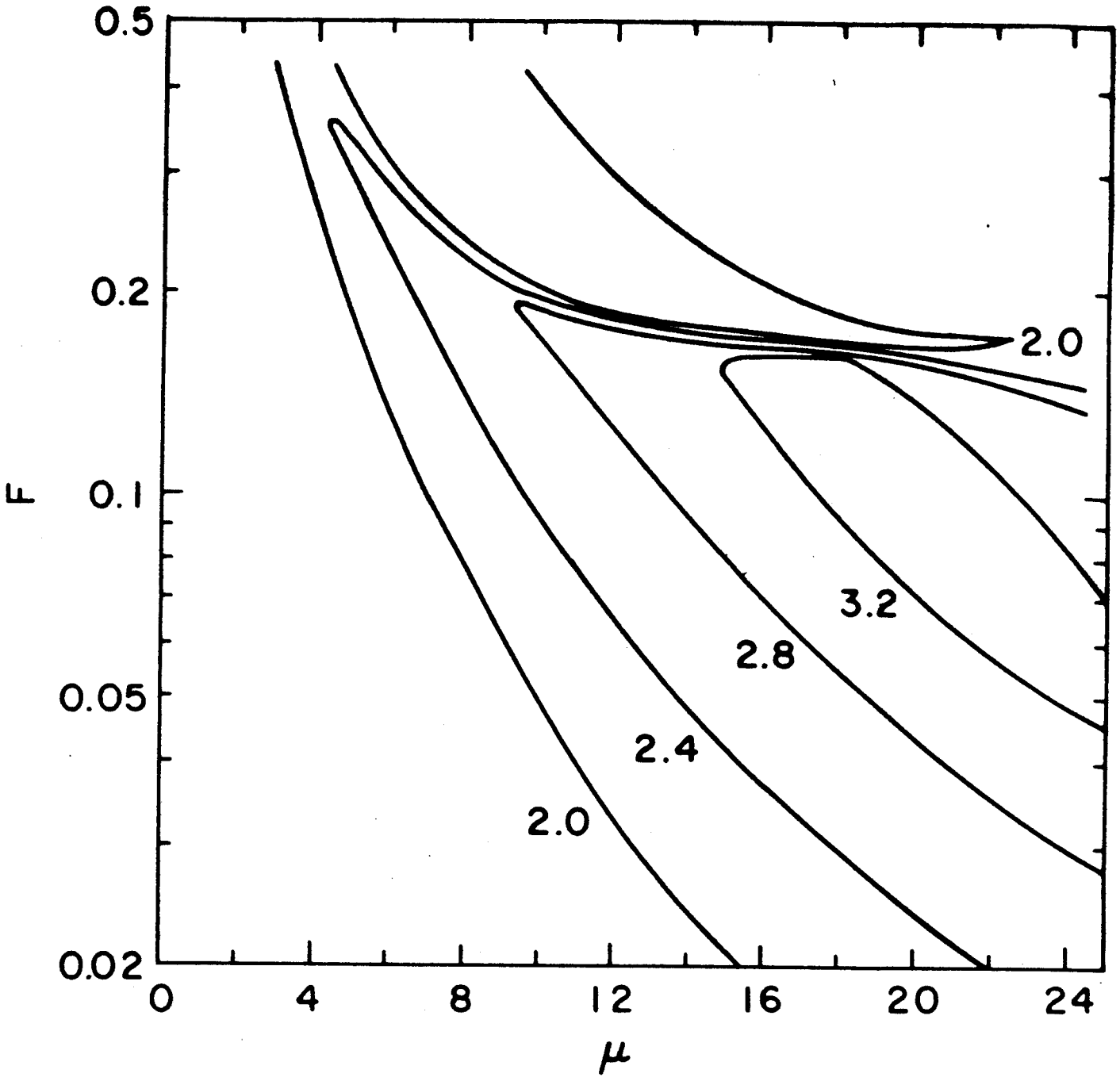

Figure 1c

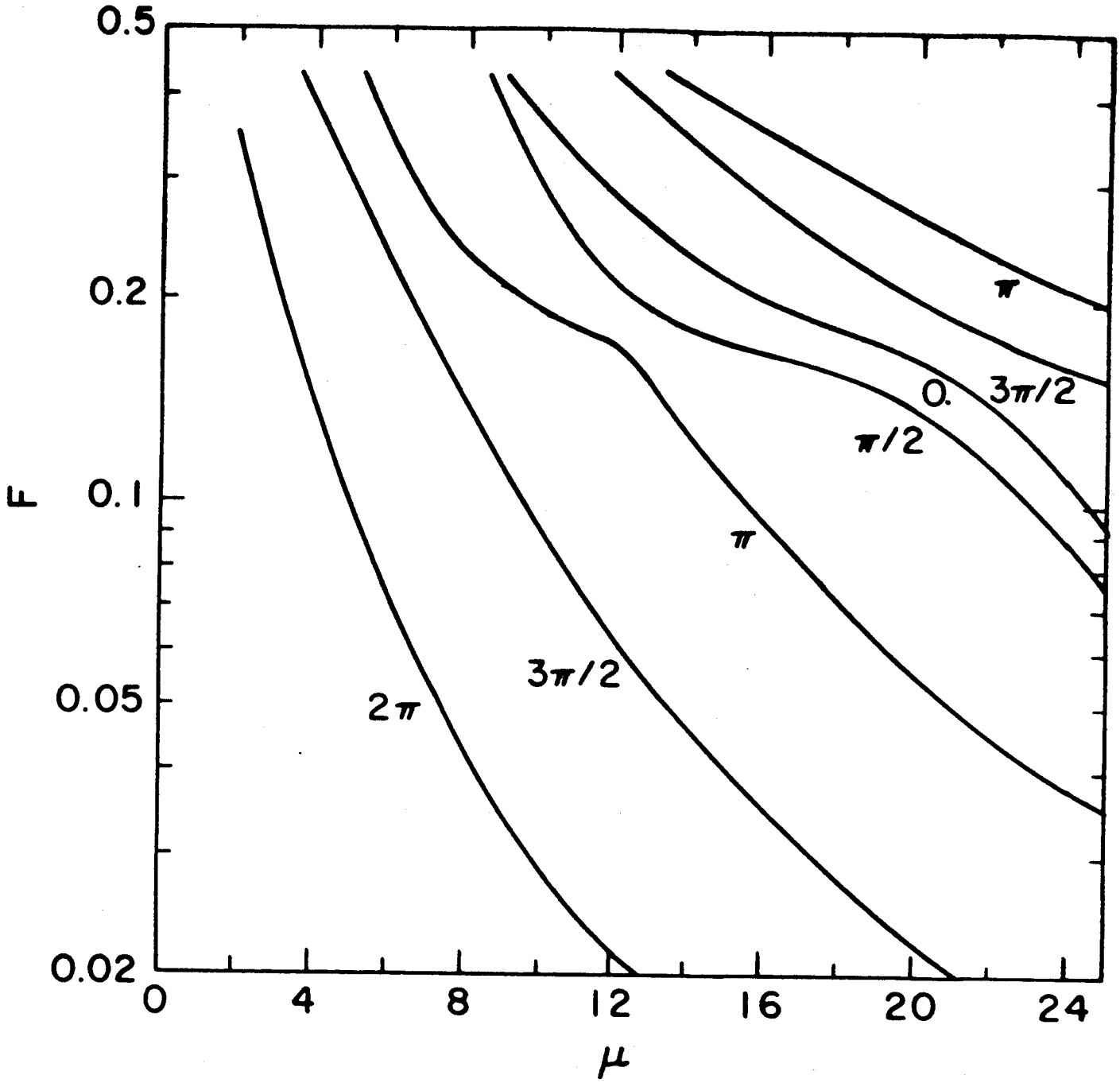

Figure 1d

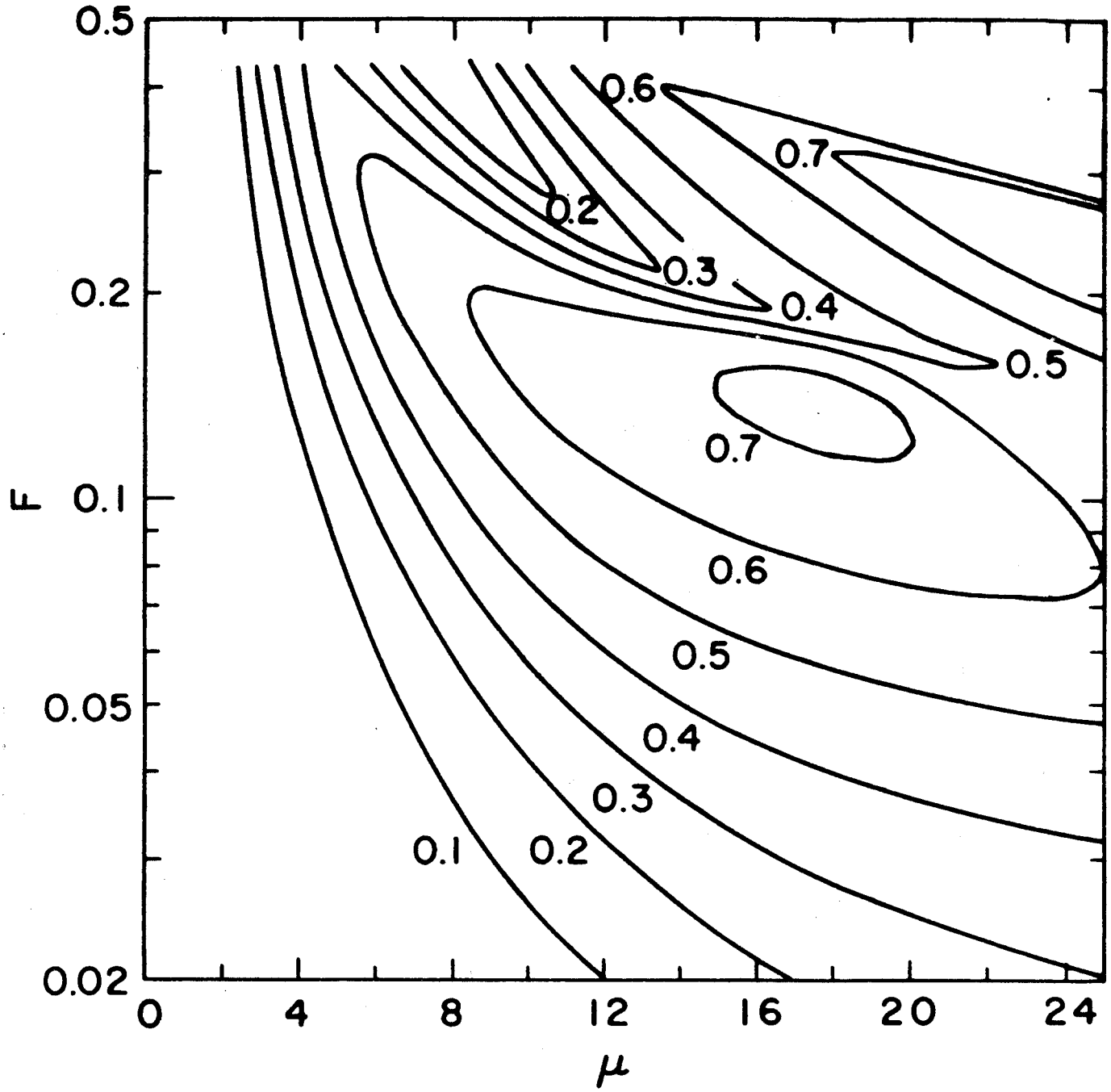
0.5
0.2
0.1
0.05
0.02
F
0
4
8
12
16
20
24
μ
0.6
0.7
0.2
0.3
0.4
0.5
0.7
0.6
0.5
0.4
0.3
0.1
0.2

Figure 2

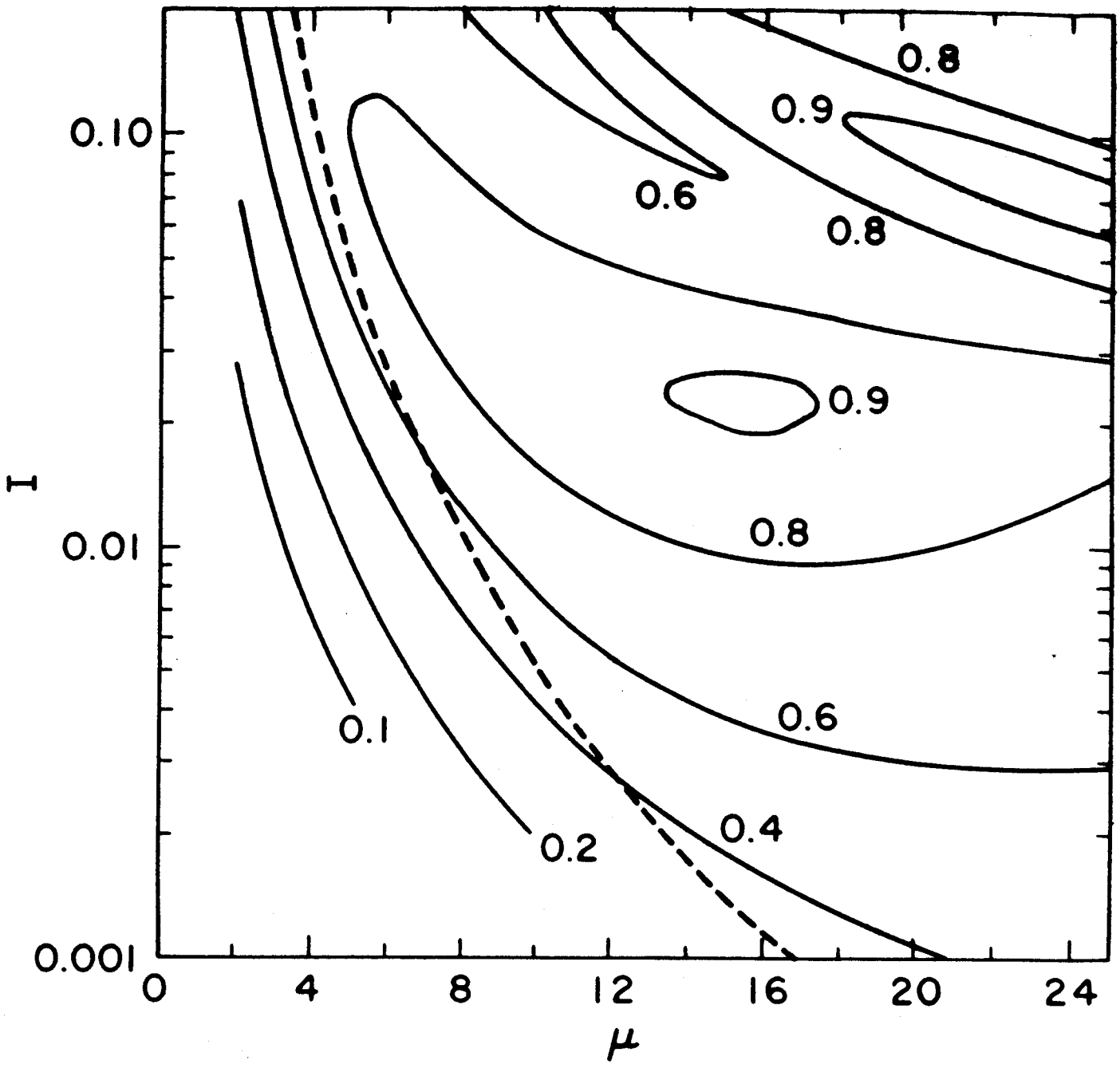

Figure 3